ChemComm

COMMUNICATION

View Article Online
View Journal | View Issue



Cite this: *Chem. Commun.*, 2014, **50**, 6714

Received 27th March 2014,
Accepted 5th May 2014

DOI: 10.1039/c4cc02273d

www.rsc.org/chemcomm

# Regulative peroxidase activity of DNA-linked hemin by graphene oxide for fluorescence DNA sensing†

Quanbo Wang, Nan Xu, Jianping Lei and Huangxian Ju*

**The inhibition effect of graphene oxide toward the peroxidase activity of DNA-linked hemin was identified and conveniently utilized in the design of a homogenous fluorescence strategy for DNA sensing with high sensitivity.**

As an active cofactor for a variety of natural enzymes such as horseradish peroxidase and catalase, Fe(III)-protoporphyrin IX (hemin) has attracted extensive research interest for mimicking catalysis in numerous applications.[1] In particular, the regulation of its catalytic activity is very important for obtaining tunable detection signals and achieving high analytical sensitivity. For example, after hemin binds with the guanine quadruplex to form a DNAzyme, the peroxidase activity of hemin can be greatly enhanced compared with that of free hemin.[2] The DNAzyme is frequently used as a signal amplifying label to develop optical or electronic biosensors for DNA/RNA, proteins, and metal ions.[3] To more efficiently utilize the catalytic function of hemin, there is an urgent need to seek an effective way to reversibly regulate the catalytic activity of hemin.

Recently, graphene has been identified as a useful carrier to load hemin for enhancing its catalytic properties.[4] The hemin–graphene hybrid can be prepared by the direct assembly of hemin on graphene with π–π interaction.[4a] Interestingly, graphene oxide (GO) cannot improve the catalytic activity of hemin due to its damaged structure.[4d] Through the chemical reduction of GO, the enhancement properties of graphene can be recovered.[5] However, the low water-solubility of graphene or reduced GO and the irreversible assembly of hemin limit its application in bioanalysis.

DNA-linked hemin can provide a feasible way to control the attachment/detachment of hemin on the GO surface according to the different affinities of GO toward single-stranded DNA (ssDNA) and double-stranded DNA (dsDNA).[6] Furthermore, hemin can catalyze a non-fluorescent substrate to form a fluorescent product in the presence of hydrogen peroxide ($H_2O_2$),[7] which thus provides the possibility of amplifying the detection signal in a "one target to multiple signal molecules" manner. This work designed a hemin labeled DNA probe (Table S1, ESI†) and demonstrated the regulative peroxidase activity of DNA-linked hemin by GO. The tunable catalysis activity could be conveniently utilized to develop a simple homogenous fluorescence strategy for a highly sensitive detection of DNA.

The hemin labeled DNA probe was synthesized *via* an amide reaction in aqueous solution, and was characterized using mass spectroscopy (Fig. S1, ESI†) and high-performance liquid chromatography (Fig. S2, ESI†). As shown in Scheme 1A, the probe could be absorbed on the GO surface due to its flexible structure and the π–π interaction between GO and the exposed nucleotide bases of ssDNA, which brought hemin to the GO surface and inhibited its catalytic property. The observed inhibiting effect of GO was

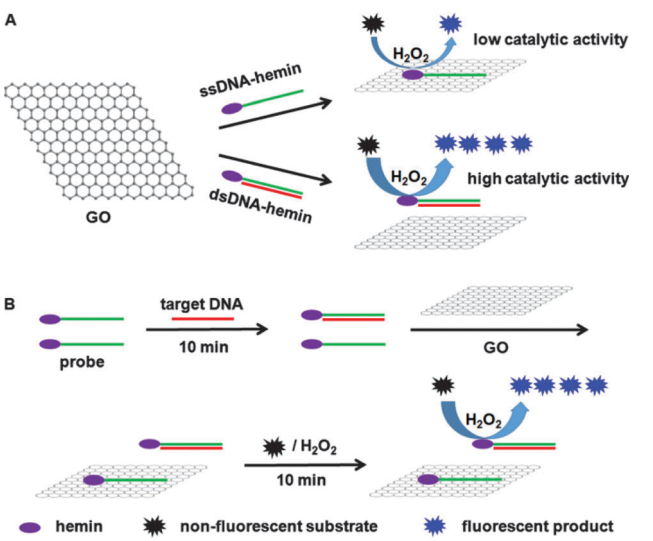


Scheme 1 Schematic illustration of (A) inhibition effect of GO toward peroxidase activity of ssDNA- or dsDNA-linked hemin, and (B) homogenous fluorescence strategy for DNA detection.

*State Key Laboratory of Analytical Chemistry for Life Science, School of Chemistry and Chemical Engineering, Nanjing University, Nanjing 210093, P. R. China. E-mail: hxju@nju.edu.cn; Fax: +86 25 83593593; Tel: +86 25 83593593*

† Electronic supplementary information (ESI) available: Experimental details and additional figures. See DOI: 10.1039/c4cc02273d

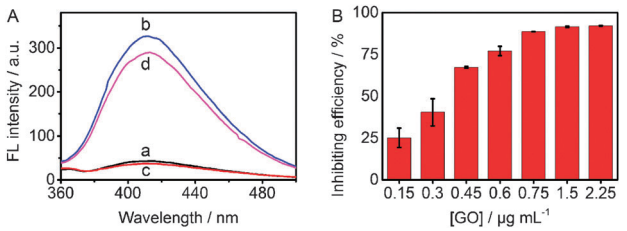


Fig. 1 (A) Fluorescent spectra of oxidation product of tyramine catalyzed by 10 nM hemin (a), probe (b), probe/GO (c) for 10 min, and probe for 10 min following by mixing with 0.75 μg $mL^{-1}$ GO (d). (B) Effect of GO concentration on its inhibiting efficiency. The catalytic reaction is carried out in 50 mM Tris-HCl (pH 7.4, containing 300 mM NaCl) with 0.7 mM tyramine and 2 mM $H_2O_2$.

reversible, and could be relieved by hybridizing the probe with a complementary DNA target to detach the formed dsDNA and thus the linked hemin from the GO surface. Based on this discrimination, a homogenous fluorescence DNA sensing strategy with high sensitivity was conveniently developed (Scheme 1B).

To verify the feasibility of the proposed method, tyramine was used as a non-fluorescent substrate, which could be catalytically oxidized into a fluorescent dimeric phenol product *via* the peroxidase activity of the probe in the presence of $H_2O_2$ (Scheme S1A, ESI†). Compared with the weak fluorescence (FL) signal catalyzed by free hemin (Fig. 1A, curve a), the fluorescence signal catalyzed by the probe was 7.3 times higher (Fig. 1A, curve b). This phenomenon could be attributed to the fact that hemin possesses weak solubility in aqueous solution, which led to its self-aggregation and lowered the peroxidase activity,[4a] while the grafting of hemin with ssDNA improved its solubility and thus excluded the aggregation to produce high peroxidase activity.[8] Further, when the probe was absorbed onto the GO surface, the catalytic fluorescence signal was significantly suppressed with a decrease of 88.5% (Fig. 1A, curve c). The signal inhibition could be attributed to two reasons that are as follows: GO possessed a strong quenching effect on the fluorescence of the catalyzed product, and the peroxidase activity of hemin was inhibited after it was absorbed on GO. To clarify this phenomenon, a control experiment was carried out by adding GO to the product of the catalytic reaction. In this case, the decrease of fluorescence intensity was attributed to only the fluorescent quenching effect of GO, which showed a signal decrease of 11.5% (Fig. 1A, curve d). Therefore, the inhibition of peroxidase activity of hemin by GO in this system was mainly responsible for the decrease of the fluorescent signal. The inhibition effect could be attributed to the decreasing diffusion rate of the probe after absorption on GO, the steric hindrance effect of GO and the possible interaction of GO with the oxidation intermediate. The latter could be concluded by the effect of GO concentration on its inhibiting efficiency. With the increasing GO concentration, the inhibiting efficiency increased and reached a plateau at 0.75 μg $mL^{-1}$ (Fig. 1B), indicating that the peroxidase activity of DNA-linked hemin could be regulated by changing the GO concentration.

To clarify the inhibition efficiency of GO toward the peroxidase activity of the probe, the 2′,7′-dichlorodihydrofluorescein diacetate ($H_2$DCFDA) as the non-fluorescent substrate was involved in this system. This compound could be catalytically oxidized into fluorescent 2′,7′-dichlorofluorescein in the presence of $H_2O_2$ (Scheme S1B, ESI†). Although the catalytic fluorescent signal was also inhibited by GO, the inhibiting efficiency of 57.1% was lower than in the case of tyramine even at a 20 times higher GO concentration of 15 μg $mL^{-1}$ (Fig. S3, ESI†). The different inhibition effects of GO could be explained as shown in Scheme S2 (ESI†). After GO absorbed the hemin labelled ssDNA probe through π–π interaction between ssDNA and GO, hemin would be brought to the hydrophobic π-conjugated carbon structures in the center of GO.[9] Compared with tyramine, $H_2$DCFDA has a larger π-conjugated structure with more hydrophobic property, which allowed easier access to hemin absorbed on the GO surface. Thus GO exhibited a more remarkable inhibition effect for tyramine than $H_2$DCFDA.

The inhibiting efficiency of tyramine depended on the pH of the reaction buffer. Although the inhibiting efficiency increased with decreasing pH from 9.0 to 6.5 (Fig. 2A), the probe showed the highest catalytic fluorescent signal at pH 7.4 (Fig. S4, ESI†). Thus pH 7.4 was chosen as the optimal value for the next experiments. The inhibiting efficiency on catalytic fluorescent signal also depended on the salt concentration of the buffer. As shown in Fig. 2B, with the increasing NaCl concentration, the inhibiting efficiency increased and reached a maximum at 300 mM. A higher concentration of $Cl^-$ led to the axial coordination between $Fe^{3+}$ and $Cl^-$, and thus slightly lowered peroxidase activity of hemin. Both low pH and high NaCl concentration were in favour of minimization of the electrostatic repulsion between the negatively charged probe and GO, thus resulting in the closer contact between labeled hemin and GO as well as intense peroxidase activity inhibition by GO. High concentrations of tyramine and $H_2O_2$ slightly decreased the inhibiting efficiency due to the limited amount of probe/GO and the maximum efficiency was achieved at 0.7 mM tyramine and 2 mM $H_2O_2$ (Fig. 2C and D).

The catalytic property of the hemin labeled ssDNA probe was further investigated by recording fluorescence kinetic curves. After adding tyramine and $H_2O_2$ to initiate the catalytic reaction,

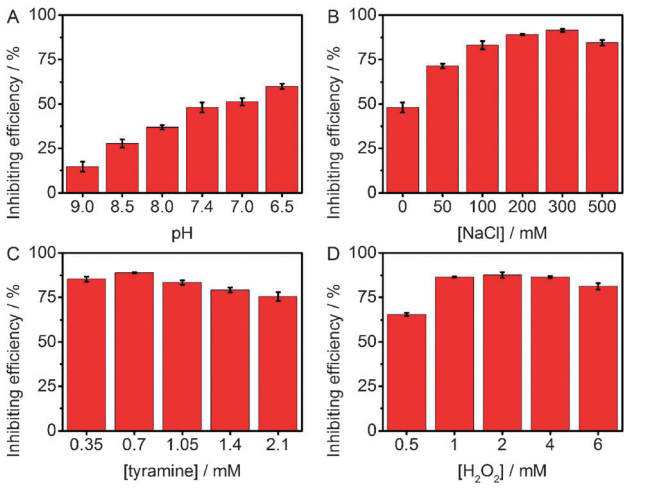


Fig. 2 Effects of (A) pH, (B) NaCl, (C) tyramine and (D) $H_2O_2$ concentration on inhibiting efficiency of GO toward fluorescent signal of oxidation product catalyzed by the probe. The concentration of probe and GO is 10 nM and 0.75 μg $mL^{-1}$, respectively.

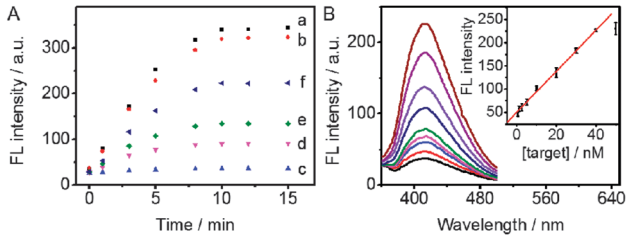


Fig. 3 (A) Fluorescence kinetic curves of the catalytic reaction for 10 nM probe (a), probe/target duplex (b), probe/GO (c) and probe/target/GO at target concentrations of 10 (d), 20 (e) and 40 nM (f). (B) Fluorescent spectra at 0, 0.5, 1.3, 2.5, 5.0, 10, 20, 30 and 40 nM target (from bottom to top). Inset: calibration curve.

the fluorescent signal of the oxidation product catalyzed by probe or probe/target duplex increased obviously and reached a plateau at 10 minutes (Fig. 3A, curves a and b), indicating that hybridization with the target would barely affect the peroxidase activity of the probe. When GO was introduced to interact with the probe, the fluorescent signal catalyzed by probe/GO was greatly suppressed (Fig. 3A, curve c). However, when the probe was first hybridized with target DNA from 10 to 40 nM and then GO was added, the fluorescence signal catalyzed by the probe enhanced gradually (Fig. 3A, curves d–f). This change could be attributed to the weaker affinity of GO to dsDNA than ssDNA due to the rigid duplex structure and the shield of the phosphate backbone on the nucleotide bases, thus weakening the interaction between hemin labelled dsDNA and GO, and the inhibition effect of GO.

The interaction between the probe or probe/target duplex and GO was demonstrated using gel electrophoresis. As shown in Fig. S5 (ESI†), the probe displayed only one band in the gel (lane a). After interaction with GO, the probe/GO did not show an obvious band (lane b) because the probe was absorbed by GO to form the probe/GO, which could hardly penetrate into the gel due to the large steric hindrance of GO.[10] However, when the probe was first hybridized with target and then mixed with GO, the probe/target duplex exhibited a slow-moving band (lane c), suggesting that the hybridization of the target with probe led to the detachment of the probe from GO.

The different inhibition effects of GO toward the peroxidase activity of ssDNA- and dsDNA-linked hemin offered an opportunity to design a novel homogeneous fluorescence DNA sensing strategy. GO was usually used as fluorescence quencher in conventional fluorescence DNA sensing strategies,[6] and theoretically one target DNA could only recover the fluorescence of one fluorophore labeled on the probe (Scheme S3, ESI†). In our strategy, GO was utilized to inhibit the peroxidase activity of hemin labeled on the probe, thus theoretically one target DNA could recover the peroxidase activity of one hemin, and then hemin could catalyze the reaction of dozens of non-fluorescent substrates to form fluorescent products, leading to fluorescent signal amplification (Scheme 1A). The DNA sensing protocol was designed by measuring the fluorescent signal catalyzed by the probe after being mixed with its complementary target in the presence of GO (Scheme 1B). The hybridization time for the probe and target was optimized to be 10 min (Fig. S6A, ESI†), and the GO concentration was optimized to be 0.75 μg $mL^{-1}$ (Fig. S6B, ESI†). Under the optimized conditions, the FL intensity was proportional to the target concentration ranging from 0.5 to 40 nM (Fig. 3B). The linear regression equation was $I = 50.6 + 4.40 \times c$ ($R$ = 0.9985), where $I$ is the FL intensity, and $c$ is the target concentration. The detection limit was estimated at $3\sigma$, which was calculated in the absence of the target for five parallel detections, to be 0.2 nM. The detection limit was 60 times lower than that in our previous work using GO and CdTe QDs as the fluorescent quencher and emitter for DNA sensing,[11] and also lower than those of previously reported homogeneous fluorescence DNA sensing strategies using GO or other nanomaterials as fluorescent quenchers (Table S2, ESI†).[12] The specificity of the protocol was demonstrated to be acceptable for discriminating the single- and three-base mismatched DNA from the complementary target (Fig. S7, ESI†).

This work identified the inhibition effect of GO toward the peroxidase activity of DNA-linked hemin and developed a simple homogenous fluorescence strategy for the highly sensitive detection of DNA. The inhibition effect of GO toward the peroxidase activity of DNA-linked hemin could be mainly attributed to the decreasing diffusion rate of the probe, the steric hindrance of GO, the interaction of GO with the oxidation intermediate, and the hydrophobicity of π-conjugated GO center. The tunable peroxidase activity of DNA-linked hemin was realized by hybridizing the probe with target DNA, which led to a homogeneous fluorescence DNA sensing strategy with high sensitivity and acceptable specificity. This catalytic fluorescence strategy was simple, relatively quick, and could be conveniently combined with other signal amplification steps for further improving the sensitivity. Also, the proposed inhibition effect could be easily extended to design other analytical applications.

This research was financially supported by the National Basic Research Program of China (2010CB732400), and the National Natural Science Foundation of China (21135002, 21121091).

## Notes and references

1 (*a*) G. I. Berglund, G. H. Carlsson, A. T. Smith, H. Szöke, A. Henriksen and J. Hajdu, *Nature*, 2002, **417**, 463–468; (*b*) Q. G. Wang, Z. M. Yang, M. L. Ma, C. K. Chang and B. Xu, *Chem. – Eur. J.*, 2008, **14**, 5073–5078; (*c*) Z. Y. Chen, L. Xu, Y. Liang and M. P. Zhao, *Adv. Mater.*, 2010, **22**, 1488–1492.

2 (*a*) P. Travascio, Y. F. Li and D. Sen, *Chem. Biol.*, 1998, **5**, 505–517; (*b*) D. Sen and L. C. H. Poon, *Crit. Rev. Biochem. Mol. Biol.*, 2011, **46**, 478–492.

3 (*a*) I. Willner, B. Shlyahovsky, M. Zayats and B. Willner, *Chem. Soc. Rev.*, 2008, **37**, 1153–1165; (*b*) Y. Xiao, V. Pavlov, T. Niazov, A. Dishon, M. Kotler and I. Willner, *J. Am. Chem. Soc.*, 2004, **126**, 7430–7431; (*c*) M. G. Deng, D. Zhang, Y. Y. Zhou and X. Zhou, *J. Am. Chem. Soc.*, 2008, **130**, 13095–13102; (*d*) Y. Y. Zhao, L. Zhou and Z. Tang, *Nat. Commun.*, 2013, **4**, 1493; (*e*) M. Luo, X. Chen, G. H. Zhou, X. Xiang, L. Chen, X. H. Ji and Z. K. He, *Chem. Commun.*, 2012, **48**, 1126–1128; (*f*) N. N. Yang, Y. Cao, P. Han, X. J. Zhu, L. Z. Sun and G. X. Li, *Anal. Chem.*, 2012, **84**, 2492–2497; (*g*) S. F. Liu, C. F. Wang, C. X. Zhang, Y. Wang and B. Tang, *Anal. Chem.*, 2013, **85**, 2282–2288.

4 (*a*) T. Xue, S. Jiang, Y. Q. Qu, Q. Su, R. Cheng, S. Dubin, C.-Y. Chiu, R. Kaner, Y. Huang and X. F. Duan, *Angew. Chem., Int. Ed.*, 2012, **51**, 3822–3825; (*b*) T. Xue, B. Peng, M. Xue, X. Zhong, C.-Y. Chiu, S. Yang, Y. Q. Qu, L. Y. Ruan, S. Jiang, S. Dubin, R. B. Kaner, J. I. Zink, M. E. Meyerhoff, X. F. Duan and Y. Huang, *Nat. Commun.*, 2014, **5**, 3200; (*c*) Y. J. Guo, L. Deng, J. Li, S. J. Guo, E. K. Wang and S. J. Dong, *ACS Nano*, 2011, **5**, 1282–1290; (*d*) Y. J. Song, Y. Chen, L. Y. Feng, J. S. Ren and X. G. Qu, *Chem. Commun.*, 2011, **47**, 4436–4438.

 

5 W. W. Tu, J. P. Lei, S. Y. Zhang and H. X. Ju, *Chem. – Eur. J.*, 2010, **16**, 10771–10777.
6 (*a*) C. H. Lu, H. H. Yang, C. L. Zhu, X. Chen and G. N. Chen, *Angew. Chem., Int. Ed.*, 2009, **48**, 4785–4787; (*b*) S. J. He, B. Song, D. Li, C. F. Zhu, W. P. Qi, Y. Q. Wen, L. H. Wang, S. P. Song, H. P. Fang and C. H. Fan, *Adv. Funct. Mater.*, 2010, **20**, 453–459; (*c*) Z. W. Tang, H. Wu, J. R. Cort, G. W. Buchko, Y. Y. Zhang, Y. Y. Shao, I. A. Aksay, J. Liu and Y. H. Lin, *Small*, 2010, **6**, 1205–1209; (*d*) H. Jang, Y.-K. Kim, H.-M. Kwon, W.-S. Yeo, D.-E. Kim and D.-H. Min, *Angew. Chem., Int. Ed.*, 2010, **49**, 5703–5707; (*e*) X. Q. Liu, F. Wang, R. Aizen, O. Yehezkeli and I. Willner, *J. Am. Chem. Soc.*, 2013, **135**, 11832–11839.
7 S. Nakayama and H. O. Sintim, *Mol. BioSyst.*, 2010, **6**, 95–97.
8 S. Nakayama, J. X. Wang and H. O. Sintim, *Chem. – Eur. J.*, 2011, **17**, 5691–5698.
9 (*a*) W. Gao, L. B. Alemany, L. J. Ci and P. M. Ajayan, *Nat. Chem.*, 2009, **1**, 403–408; (*b*) K. P. Loh, Q. L. Bao, G. Eda and M. Chhowalla, *Nat. Chem.*, 2010, **2**, 1015–1024.
10 J. H. Liu, C. Y. Wang, Y. Jiang, Y. P. Hu, J. S. Li, S. Yang, Y. H. Li, R. H. Yang, W. H. Tan and C. Z. Huang, *Anal. Chem.*, 2013, **85**, 1424–1430.
11 H. F. Dong, W. C. Gao, F. Yan, H. X. Ji and H. X. Ju, *Anal. Chem.*, 2010, **82**, 5511–5517.
12 (*a*) L. Cui, X. Y. Lin, N. H. Lin, Y. L. Song, Z. Zhu, X. Chen and C. J. Yang, *Chem. Commun.*, 2012, **48**, 194–196; (*b*) L. B. Zhang, S. J. Guo, S. J. Dong and E. K. Wang, *Anal. Chem.*, 2012, **84**, 3568–3573; (*c*) C. F. Zhu, Z. Y. Zeng, H. Li, F. Li, C. H. Fan and H. Zhang, *J. Am. Chem. Soc.*, 2013, **135**, 5998–6001; (*d*) X. Zhu, H. Y. Zheng, X. F. Wei, Z. Y. Lin, L. H. Guo, B. Qiu and G. N. Chen, *Chem. Commun.*, 2013, **49**, 1276–1278; (*e*) Q. B. Wang, W. Wang, J. P. Lei, N. Xu, F. L. Gao and H. X. Ju, *Anal. Chem.*, 2013, **85**, 12182–12188.